

# Unifying Reactive Collision Avoidance and Control Allocation for Multi-Vehicle Systems\*

Josef Matouš, Erlend A. Basso, Emil H. Thyri, and Kristin Y. Pettersen

**Abstract**—To enable autonomous vehicles to operate in cluttered and unpredictable environments with numerous obstacles, such vehicles need a collision avoidance system that can react to and handle sudden changes in the environment. In this paper, we propose an optimization-based reactive collision avoidance system that uses control barrier functions integrated into the control allocation. We demonstrate the effectiveness of our method through numerical simulations with autonomous surface vehicles. The simulated vehicles track their reference waypoints while maintaining safe distances. The proposed method can be readily implemented on vehicles that already use an optimization-based control allocation method.

## I. INTRODUCTION

Autonomous vehicles are being increasingly used in cluttered and unpredictable environments where considerations to other vehicles and obstacles need to be made. Therefore, the control system of autonomous vehicles should include some form of collision avoidance (COLAV).

Reviews of various COLAV concepts are presented in [1]–[3]. In general, algorithms for COLAV can be split into two categories: motion planning and reactive algorithms.

Motion planning algorithms include, among others, various types of path planning algorithms [4]–[6], the dynamic window algorithm [7], and model predictive control (MPC). MPC can be used both for a single vehicle [8], [9] and for multi-agent systems in a distributed form [10], [11].

Reactive algorithms for COLAV include, among others, virtual potential fields [12], geometric guidance [13], and control barrier functions (CBFs) [14]–[18]. Reactive algorithms are often used together with motion planning algorithms in a hybrid controller. In such a controller, the reactive algorithm ensures the safety of the vehicle in unexpected situations. Such an algorithm is proposed in [19], where a collision-free velocity reference is obtained through numerical optimization. The proposed algorithm is designed specifically for autonomous surface vehicles (ASVs).

CBFs offer a COLAV method that is applicable for a wide range of systems [20]. In the literature, there are typically two ways in which CBFs are applied for COLAV. They are either applied to a simplified model of the vehicle (*e.g.*, a unicycle model [14], [15]) to provide safe velocity references, or they

are used together with control Lyapunov functions (CLFs) [16]–[18] on the complete model.

Reactive COLAV methods that work with a simplified model do not take into account the physical limitations of the vehicle, such as acceleration or actuator constraints. Consequently, these methods may output reference signals that the underlying controllers cannot track. To mitigate this, reactive COLAV methods should be included into the lowest-possible control level.

In this paper, we consider overactuated vehicles, *i.e.*, vehicles with more actuators than degrees of freedom (DOFs), with a control system consisting of blocks shown in Figure 1. The control system contains a long-term, deliberate planner, a high-level controller that outputs desired forces and torques ( $\tau_d$ ), and a control allocation block. The goal of control allocation is to find actuator control inputs ( $\mathbf{u}$ ) that generate the desired forces and torques. Most control allocation methods are based on numerical optimization [21]–[23] which makes them ideal for augmenting with CBF constraints.

The main contribution of this paper is a reactive COLAV algorithm that is included at the lowest level in the control pipeline, *i.e.* in the control allocation, to ensure the safety of the vehicle regarding collision avoidance. Since it is included at the lowest-possible control level, it also ensures the “baseline” safety of any other higher level (long term/deliberate) planners of the vehicle guidance, navigation and control system. The algorithm can easily be implemented on vehicles that apply a numerical optimization-based method to control allocation. Moreover, the algorithm does not rely on any communication between the vehicles; the only required information is the position and velocity of other vehicles. The paper extends the results in [24], which only considers ASVs and simple encounters between one ASV and a vessel moving at a constant course and speed, making the method applicable to a wider range of vehicles and scenarios with multiple autonomous vehicles.

The remainder of the paper is organized as follows. Section II defines the notation and describes the model of the vehicle. The proposed control allocation method and CBFs for COLAV are introduced in Sections III and IV. Section V describes the resulting combined COLAV and control allocation optimization problem. Section VI presents the results of numerical simulations using models of ASVs.

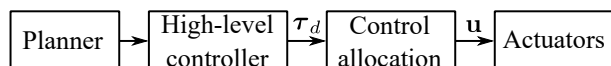


Fig. 1: Control system of overactuated vehicles considered in this paper

\*This work was partly supported by the Research Council of Norway through project No. 302435 and the Centres of Excellence funding scheme, project No. 223254.

The authors are with the Centre for Autonomous Marine Operations and Systems (AMOS), Department of Engineering Cybernetics, Norwegian University of Science and Technology (NTNU), NO-7491, Trondheim, Norway {josef.matous, erlend.a.basso, emil.h.thyri, kristin.y.pettersen}@ntnu.no

Finally, Section VII contains some concluding remarks.

## II. VEHICLE MODEL

### A. Notation

Let  $\mathbf{p}$  denote the position and  $\Theta$  the orientation (expressed using the Euler angles) of the vehicle in a North-East-Down (NED) reference frame. Let  $\boldsymbol{\eta}$  be the pose of the vehicle

$$\boldsymbol{\eta} = \begin{bmatrix} \mathbf{p}^T, \Theta^T \end{bmatrix}^T. \quad (1)$$

Let  $\boldsymbol{\nu}$  be the velocities of the vehicle in the body-centered frame. The complete state of the vehicle,  $\mathbf{x}$ , is defined as

$$\mathbf{x} = \begin{bmatrix} \boldsymbol{\eta}^T, \boldsymbol{\nu}^T \end{bmatrix}^T. \quad (2)$$

Let  $\boldsymbol{\tau}$  be the vector of generalized forces acting on the vehicle. Let  $K$  be the number of actuator parameters and  $\mathbf{u} \in \mathbb{R}^K$  the vector of inputs. Furthermore, let  $b : \mathbb{R}^K \rightarrow \mathbb{R}^{n_{\text{DOF}}}$  be a nonlinear function that maps the inputs to the generalized forces ( $n_{\text{DOF}}$  is the number of DOFs).

### B. Equations of Motion

The time-derivative of the pose can be obtained by transforming the velocities. In addition, we assume that the time-derivatives of the velocities are affine in the generalized forces. We thus consider vehicles described by the following dynamical equations

$$\dot{\boldsymbol{\eta}} = \begin{bmatrix} \dot{\boldsymbol{\eta}} \\ \dot{\boldsymbol{\nu}} \end{bmatrix} = \begin{bmatrix} \mathbf{J}(\Theta) \boldsymbol{\nu} \\ f(\mathbf{x}) + g(\mathbf{x}) \boldsymbol{\tau} \end{bmatrix} = \begin{bmatrix} \mathbf{J}(\Theta) \boldsymbol{\nu} \\ f(\mathbf{x}) + g(\mathbf{x}) b(\mathbf{u}) \end{bmatrix}, \quad (3)$$

where  $\mathbf{J}(\Theta)$  is the transformation matrix. This equation describes a large class of systems, including the matrix-vector model of marine vessels [25]

$$\dot{\boldsymbol{\eta}} = \mathbf{J}(\Theta) \boldsymbol{\nu}, \quad (4a)$$

$$\mathbf{M} \dot{\boldsymbol{\nu}} + (\mathbf{C}(\boldsymbol{\nu}) + \mathbf{D}(\boldsymbol{\nu})) \boldsymbol{\nu} + \mathbf{g}(\boldsymbol{\eta}) = b(\mathbf{u}), \quad (4b)$$

where  $\mathbf{M}$ ,  $\mathbf{C}(\boldsymbol{\nu})$  and  $\mathbf{D}(\boldsymbol{\nu})$  is the mass, Coriolis and drag matrix, respectively. This model can be converted to the form in (3) since the matrix  $\mathbf{M}$  is invertible.

## III. CONTROL ALLOCATION

As stated in the Introduction, the goal of the control allocation is to find the inputs that generate the desired forces given by the high-level controller. For details on control allocation techniques for both linear and nonlinear systems, the reader is referred to [26].

In this paper, we consider systems where the function  $b$  can be nonlinear. In the literature, nonlinear control allocation is commonly solved by linearizing the function  $b$  [22], [23]

$$b(\mathbf{u}_0 + \Delta \mathbf{u}) \approx b(\mathbf{u}_0) + \mathbf{B}(\mathbf{u}_0) \Delta \mathbf{u}, \quad (5)$$

where  $\mathbf{u}_0$  are the inputs around which we linearize,  $\Delta \mathbf{u}$  is the increment, and

$$\mathbf{B}(\mathbf{u}_0) = \left. \frac{\partial b(\mathbf{u})}{\partial \mathbf{u}} \right|_{\mathbf{u}_0}, \quad (6)$$

is the Jacobian of  $b$  evaluated at  $\mathbf{u}_0$ . Let  $\boldsymbol{\tau}_d$  be the desired forces. The goal of our control allocation scheme is to find optimal inputs  $\mathbf{u}^*$  that satisfy

$$\mathbf{u}^* = \arg \min_{\mathbf{u} \in \mathbb{R}^K} \|b(\mathbf{u}) - \boldsymbol{\tau}_d\|^2, \quad (7)$$

where  $\|\cdot\|$  is the Euclidean norm.

Using the approximation (5), we can formulate the control allocation problem as a quadratic program (QP)

$$\mathbf{u}^* = \mathbf{u}_0 + \Delta \mathbf{u}^*, \quad (8)$$

$$\Delta \mathbf{u}^* = \arg \min_{\Delta \mathbf{u} \in \mathbb{R}^K} \|b(\mathbf{u}_0) + \mathbf{B}(\mathbf{u}_0) \Delta \mathbf{u} - \boldsymbol{\tau}_d\|^2. \quad (9)$$

## IV. CONTROL BARRIER FUNCTIONS

In this section, we will briefly present the theory behind control barrier functions (CBFs). For more details, the reader is referred to [20]. After presenting the notation for multiple vehicles, we define the CBF for COLAV.

### A. Introduction to CBFs

Consider a nonlinear control-affine system

$$\dot{\mathbf{x}} = \tilde{f}(\mathbf{x}) + \tilde{g}(\mathbf{x}) \mathbf{u}, \quad (10)$$

where  $\mathbf{x} \in \mathbb{R}^n$ . A barrier function  $h : \mathbb{R}^n \rightarrow \mathbb{R}$  defines a safe set

$$\mathcal{C} = \{\mathbf{x} \mid h(\mathbf{x}) \geq 0\}. \quad (11)$$

Assuming that the initial condition lies in the safe set, the system trajectory will stay within  $\mathcal{C}$  if the following inequality holds [20]

$$\frac{d}{dt} h(\mathbf{x}) = \frac{\partial h(\mathbf{x})}{\partial \mathbf{x}} \left( \tilde{f}(\mathbf{x}) + \tilde{g}(\mathbf{x}) \mathbf{u} \right) \geq -\gamma(h(\mathbf{x})), \quad (12)$$

where  $\gamma$  is an extended class- $\mathcal{K}_\infty$  function. If there exists a  $\mathbf{u}$  such that (12) is satisfied, then  $h$  is a valid CBF.

### B. CBFs for Reactive Collision Avoidance

Let there be  $m$  vehicles. We shall denote the variables that belong to a given vehicle by an upper index (e.g.,  $\mathbf{x}^i$  is the state of the  $i^{\text{th}}$  vehicle). In addition, let us define a relative position of vehicles  $i$  and  $j$  as

$$\mathbf{p}^{ij} = \mathbf{p}^i - \mathbf{p}^j. \quad (13)$$

To ensure safety, we need a collection of CBFs that enforce safe distances between each pair of vehicles. In the literature, vehicles described by the model (3) frequently use CBFs in the following form [17], [24]

$$h^{ij}(\mathbf{x}^i, \mathbf{x}^j) = \|\mathbf{p}^{ij}\| - d_{\min} + k_v \frac{d}{dt} \|\mathbf{p}^{ij}\|, \quad (14)$$

where  $d_{\min}$  is a minimum safe distance, and  $k_v$  is a coefficient that penalizes the relative speed of the vehicles.

To use  $h^{ij}$  as a control barrier function, we need to calculate its time-derivative. Differentiating (14) with respect to time yields

$$\frac{d}{dt} h^{ij}(\mathbf{x}^i, \mathbf{x}^j) = \frac{d}{dt} \|\mathbf{p}^{ij}\| + k_v \frac{d^2}{dt^2} \|\mathbf{p}^{ij}\|. \quad (15)$$

To calculate the first and second time-derivative of the relative distance, we need to find the first and second time-derivatives of the relative position. For  $\dot{\mathbf{p}}^{ij}$ , we split the derivative of  $\boldsymbol{\eta}$  from (3) into the derivatives of position and orientation

$$\dot{\boldsymbol{\eta}}^i = \begin{bmatrix} \dot{\mathbf{p}}^i \\ \dot{\boldsymbol{\Theta}}^i \end{bmatrix} = \begin{bmatrix} \mathbf{J}_p(\boldsymbol{\Theta}^i) \\ \mathbf{J}_\Theta(\boldsymbol{\Theta}^i) \end{bmatrix} \boldsymbol{\nu}^i. \quad (16)$$

Substituting this into the time-derivative of (13) yields

$$\dot{\mathbf{p}}^{ij} = \mathbf{J}_p(\boldsymbol{\Theta}^i) \boldsymbol{\nu}^i - \mathbf{J}_p(\boldsymbol{\Theta}^j) \boldsymbol{\nu}^j. \quad (17)$$

For  $\ddot{\mathbf{p}}^{ij}$ , we assume that the target maintains its velocity, *i.e.*,

$$\ddot{\mathbf{p}}^{ij} \approx \ddot{\mathbf{p}}^i, \quad (18)$$

when calculating the time-derivative for the  $i^{\text{th}}$  vehicle. As discussed in [24], this is a ‘‘mild worst-case’’ assumption, since maneuvers of the target vehicle tend to aid to resolving the situation. Thus, taking the time-derivative of (17) yields

$$\ddot{\mathbf{p}}^i = \dot{\mathbf{J}}_p(\boldsymbol{\Theta}^i) \boldsymbol{\nu}^i + \mathbf{J}_p(\boldsymbol{\Theta}^i) \dot{\boldsymbol{\nu}}^i. \quad (19)$$

Finally, we substitute the approximation of forces from (5) into the equation for  $\dot{\boldsymbol{\nu}}$  in (3) to get

$$\dot{\boldsymbol{\nu}}^i = f(\mathbf{x}^i) + g(\mathbf{x}^i) (b(\mathbf{u}_0^i) + \mathbf{B}(\mathbf{u}_0^i) \Delta \mathbf{u}^i), \quad (20)$$

which we can substitute into (19) to calculate  $\ddot{\mathbf{p}}^i$ .

## V. FORMULATING THE OPTIMIZATION PROBLEM

Now we can combine the definitions from Sections III and IV to formulate the proposed optimization problem for control allocation with multi-vehicle COLAV.

### A. The basic optimization problem

Let  $\mathbf{u}_0^i$  be the inputs of vehicle  $i$  from the previous control period. The new inputs are calculated as

$$\mathbf{u}^i = \mathbf{u}_0^i + (\Delta \mathbf{u}^i)^*, \quad (21)$$

where  $(\Delta \mathbf{u}^i)^*$  is obtained by solving the QP

$$(\Delta \mathbf{u}^i)^* = \arg \min_{\Delta \mathbf{u}^i \in \mathbb{R}^K} \|b(\mathbf{u}_0^i) + \mathbf{B}(\mathbf{u}_0^i) \Delta \mathbf{u}^i - \boldsymbol{\tau}_d^i\|^2, \quad (22a)$$

$$\text{s.t. } \frac{d}{dt} h^{ij}(\mathbf{x}^i, \mathbf{x}^j) \geq -\gamma (h^{ij}(\mathbf{x}^i, \mathbf{x}^j)), \quad (22b)$$

$$j \in \{1, \dots, m\} \setminus \{i\}, \quad (22c)$$

$$\mathbf{u}_{\min}^i \leq \mathbf{u}_0^i + \Delta \mathbf{u}^i \leq \mathbf{u}_{\max}^i, \quad (22c)$$

$$\Delta \mathbf{u}_{\min}^i \leq \Delta \mathbf{u}^i \leq \Delta \mathbf{u}_{\max}^i, \quad (22d)$$

where  $\mathbf{u}_{\min}^i$  and  $\mathbf{u}_{\max}^i$  are the absolute actuator limits, and  $\Delta \mathbf{u}_{\min}^i$  and  $\Delta \mathbf{u}_{\max}^i$  are the actuator rate limits. The absolute limits are usually given by the physical limitations of the vehicle (*e.g.*, the thrust of a propeller or the deflection of control surfaces) whereas the rate limits are user-defined to reduce the rapid changes that wear out the actuators.

Simulation results using this control allocation algorithm are presented in Section VI.

### B. Modified Optimization Problem

The algorithm in (22) is suitable for vehicles where the number of actuators is equivalent to the number of DOFs. Applying the algorithm to vehicles where the number of actuators is much greater than the number of DOFs results in inefficient usage of the available actuators, as can be seen in Section VI.

To reduce this effect, we add penalty terms on the actuator usage, similar to those proposed in [23], in the cost function. To simplify the notation, let  $\|\mathbf{x}\|_{\mathbf{Q}}^2$  be the squared norm of a vector  $\mathbf{x}$  weighted by a matrix  $\mathbf{Q}$ , *i.e.*,

$$\|\mathbf{x}\|_{\mathbf{Q}}^2 = \mathbf{x}^T \mathbf{Q} \mathbf{x}. \quad (23)$$

The modified optimization problem is defined as follows

$$(\Delta \mathbf{u}^i)^* = \arg \min_{\Delta \mathbf{u}^i \in \mathbb{R}^K} \|b(\mathbf{u}_0^i) + \mathbf{B}(\mathbf{u}_0^i) \Delta \mathbf{u}^i - \boldsymbol{\tau}_d^i\|_{\mathbf{Q}}^2 \quad (24a)$$

$$+ \|\mathbf{u}_0^i + \Delta \mathbf{u}^i\|_{\mathbf{R}_{\text{abs}}}^2 + \|\Delta \mathbf{u}^i\|_{\mathbf{R}_{\text{rel}}}^2,$$

$$\text{s.t. constraints (22b)–(22d)}, \quad (24b)$$

where  $\mathbf{Q}$  is a positive definite matrix that penalizes the difference between the desired and actual forces, and  $\mathbf{R}_{\text{abs}}$  and  $\mathbf{R}_{\text{rel}}$  are positive semidefinite matrices that penalize the absolute and incremental usage of actuators, respectively.

Note that both (22) and (24) use only local information and measurements, and can thus be solved locally.

## VI. SIMULATIONS

In the simulations, we test the ability of the proposed algorithms to resolve a situation when four surface vessels are simultaneously in danger of collision. Each vessel starts in the corner of a square and is guided towards a reference located in the diagonally opposite corner.

We tested the proposed algorithms on two models of ASVs — the *milliAmpere* ferry [27] and the 1 : 90 scaled model of the Inocean Cat I drillship [28] — using Simulink. Both vessels are equipped with azimuth thrusters; the *milliAmpere* has two and the drillship has six. Each thruster is parametrized by two values: its thrust force and its azimuth. The input vector for these vessels is defined as

$$\mathbf{u} = [f_1, \dots, f_k, \alpha_1, \dots, \alpha_k]^T, \quad (25)$$

where  $f_i$  is the thrust force and  $\alpha_i$  is the azimuth angle of the  $i^{\text{th}}$  thruster, and  $k$  is the number of thrusters. Both ASV models have 3DOFs, *i.e.*, the North-East position and the yaw angle. The function that maps the inputs to the generalized forces is

$$b(\mathbf{u}) = \sum_{i=1}^k f_i [\cos \alpha_i, \sin \alpha_i, L_x^i \sin \alpha_i - L_y^i \cos \alpha_i]^T, \quad (26)$$

where  $L_x^i$  and  $L_y^i$  is the position of the  $i^{\text{th}}$  thruster, relative to the center of mass.

For the higher-level controller that provides the desired forces, we use a nonlinear PID controller [25]. The nonlinear PID is an output-linearizing controller that transforms the nonlinear dynamical equations from (4) to

$$\ddot{\boldsymbol{\eta}} + 2 \boldsymbol{\Omega}_n \mathbf{Z} \dot{\boldsymbol{\eta}} + \boldsymbol{\Omega}_n^2 \boldsymbol{\eta} = 0, \quad (27)$$

| Scenario | Thruster utilization [%] |         |       |        |
|----------|--------------------------|---------|-------|--------|
|          | Maximum                  | Minimum | Mean  |        |
| MA       | basic                    | 2.074   | 1.550 | 1.822  |
|          | modified                 | 0.838   | 0.835 | 0.837  |
| DS       | basic                    | 100.000 | 1.282 | 51.496 |
|          | modified                 | 6.161   | 0.259 | 3.816  |

TABLE I: Steady-state thruster utilization of the *basic* algorithm (22) and the *modified* algorithm (24). MA — the *milliAmpere* vessel, DS — the *drillship* scale model

where  $\mathbf{Z}$  is the diagonal relative damping matrix, and  $\mathbf{\Omega}_n$  is the diagonal natural frequency matrix. Both matrices are tuning parameters. For convenience, we express  $\mathbf{\Omega}_n$  in terms of a bandwidth matrix  $\mathbf{\Omega}_{bw}$

$$\mathbf{\Omega}_n = \mathbf{\Omega}_{bw} \left( \sqrt{\mathbf{I} - 2\mathbf{Z}^2} + \sqrt{4\mathbf{Z}^4 - 4\mathbf{Z}^2 + 2\mathbf{I}} \right)^{-1}, \quad (28)$$

where  $\sqrt{\cdot}$  is an elementwise square root.

The simulation parameters for both vessels are summarized in Table II. The matrix  $\mathbf{Q}$  is chosen as

$$\mathbf{Q} = \text{diag} \left( 1, 1, \frac{1}{L^2} \right), \quad L = \min_i \sqrt{(L_x^i)^2 + (L_y^i)^2}. \quad (29)$$

Since the power consumption of a thruster increases with the absolute value of its thrust force and the increment of its azimuth, the matrices  $\mathbf{R}_{\text{abs}}$  and  $\mathbf{R}_{\text{rel}}$  are chosen as

$$\mathbf{R}_{\text{abs}} = \begin{bmatrix} r_{\text{abs}} \mathbf{I}_{k \times k} & \\ & \mathbf{0}_{k \times k} \end{bmatrix}, \quad \mathbf{R}_{\text{rel}} = \begin{bmatrix} \mathbf{0}_{k \times k} & \\ & r_{\text{rel}} \mathbf{I}_{k \times k} \end{bmatrix}, \quad (30)$$

where  $\mathbf{I}_{n \times n}$  is an  $n$ -by- $n$  identity matrix, and  $\mathbf{0}_{n \times n}$  is an  $n$ -by- $n$  matrix of zeros. The rate constraints are identical for all thrusters and symmetric, *i.e.*,

$$\Delta \mathbf{u}_{\text{max}} = \begin{bmatrix} \Delta f_{\text{max}} \mathbf{1}_k \\ \Delta \alpha_{\text{max}} \mathbf{1}_k \end{bmatrix}, \quad \Delta \mathbf{u}_{\text{min}} = -\Delta \mathbf{u}_{\text{max}}, \quad (31)$$

where  $\Delta f_{\text{max}}$  and  $\Delta \alpha_{\text{max}}$  are the force and azimuth rate constraints, respectively, and  $\mathbf{1}_k$  is a vector of ones.

The results of the simulations are shown in Figures 2, 3, and 4. Figure 2 shows the results of algorithm (22). Figure 3 shows the results of algorithm (24). Each figure consists of

| Parameter                          | <i>milliAmpere</i>      | <i>drillship</i>  |
|------------------------------------|-------------------------|-------------------|
| $\mathbf{\Omega}_{bw}$             | diag (0.1, 0.1, 0.5)    |                   |
| $\mathbf{Z}$                       | diag (0.95, 0.95, 0.97) |                   |
| $\mathbf{Q}$                       | diag (1, 1, 0.7)        | diag (1, 1, 1.13) |
| $r_{\text{abs}}$                   | 1                       | 1                 |
| $r_{\text{rel}}$                   | 100                     | 1                 |
| $d_{\text{min}}$ [m]               | 15                      | 2.5               |
| $k_v$ [s]                          | 15                      | 15                |
| $\gamma(h)$                        | 0.1 $h$                 | 0.1 $h$           |
| $f_{\text{min}}$ [N]               | -350                    | -0.8              |
| $f_{\text{max}}$ [N]               | 500                     | 1.5               |
| $\Delta f_{\text{max}}$ [N]        | 350                     | 0.5               |
| $\Delta \alpha_{\text{max}}$ [rad] | $\frac{\pi}{8}$         | $\frac{\pi}{8}$   |

TABLE II: Simulation parameters. Parameters  $\mathbf{\Omega}_{bw}$  and  $\mathbf{Z}$  are identical for both scenarios, diag ( $\cdot$ ) is a diagonal matrix

two plots. The plot on the left displays the trajectory of the vessels. The colored lines show the trajectory of each vessel, the boat-shaped polygons represent the pose of the vessels at several evenly spaced time-instances, and the colored crosses show the reference of each vessel. The plot on the right shows the smallest distance between the vessels compared to the minimum safe distance  $d_{\text{min}}$ . In both scenarios, the vessels reach their reference position while maintaining safe distance.

We also tested a scenario where one of the vessels is uncontrolled. The results are shown in Figure 4. In this scenario, the uncontrolled vessel (plotted in black) solves the control allocation problem without the CBF constraints (22b). Although the time it takes the vessels to converge to their goal positions is greater, the minimum safe distance is still maintained.

In this section, we have provided some insight into how to choose some of the parameters for the simulated models. When it comes to the choice of the coefficient  $k_v$ , introduced in (14), and the extended class- $\mathcal{K}_\infty$  function  $\gamma$ , introduced in (22), the following considerations can be made. Intuitively, increasing  $k_v$  increases the size of the “unsafe” region where the barrier function is negative, causing the system to react sooner in situations where two vehicles are on collision course. Conversely, increasing the slope of  $\gamma$  decreases the size of the region where the constraint (22b) is active, causing the system to react later.

## VII. CONCLUSIONS AND FUTURE WORK

In this paper, we have proposed a method for integrating a COLAV scheme into control allocation through control barrier functions. We have demonstrated its effectiveness on two models of ASVs, where it significantly improved the safety. The proposed method can be readily implemented on vehicles that already use optimization-based control allocation by simply including the constraints given by the control barrier functions in the optimization.

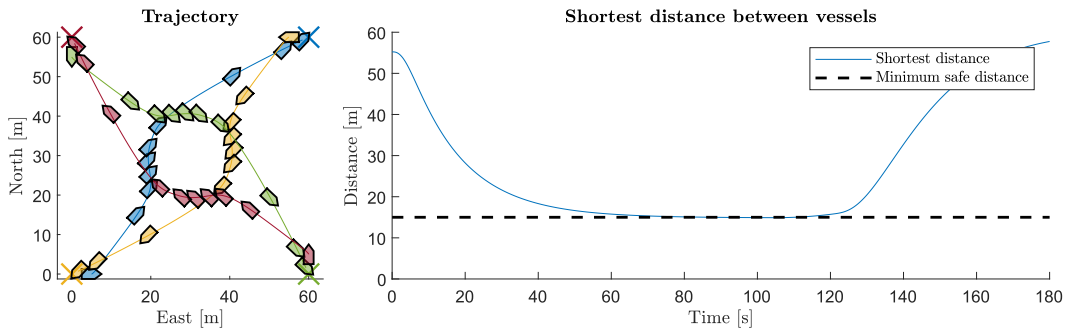
Finding a systematic method for choosing the parameter values that guarantee safety for a given vehicle model is a topic for future work.

## ACKNOWLEDGMENT

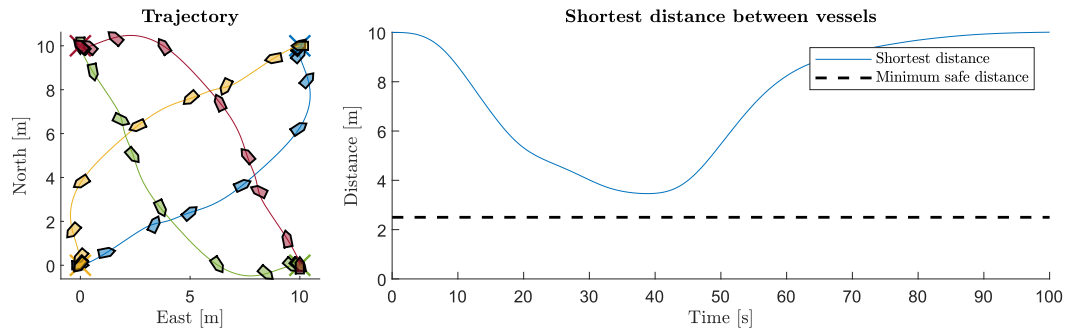
The authors would like to thank Damiano Varagnolo and Claudio Paliotta for their advice on the optimization problem and the structure of the paper.

## REFERENCES

- [1] T. Statheros, G. Howells, and K. M. Maier, “Autonomous Ship Collision Avoidance Navigation Concepts, Technologies and Techniques,” *The Journal of Navigation*, vol. 61, no. 1, pp. 129–142, Jan. 2008.
- [2] C. Tam, R. Bucknall, and A. Greig, “Review of Collision Avoidance and Path Planning Methods for Ships in Close Range Encounters,” *The Journal of Navigation*, vol. 62, no. 3, pp. 455–476, Jul. 2009.
- [3] M. Hoy, A. S. Matveev, and A. V. Savkin, “Algorithms for Collision-free Navigation of Mobile Robots in Complex Cluttered Environments: A Survey,” *Robotica*, vol. 33, no. 3, pp. 463–497, Mar. 2015.
- [4] T. Wang, X. P. Yan, Y. Wang, and Q. Wu, “Ship Domain Model for Multi-ship Collision Avoidance Decision-making with COLREGs Based on Artificial Potential Field,” *TransNav, the International Journal on Marine Navigation and Safety of Sea Transportation*, vol. 11, no. 1, pp. 85–92, 2017.

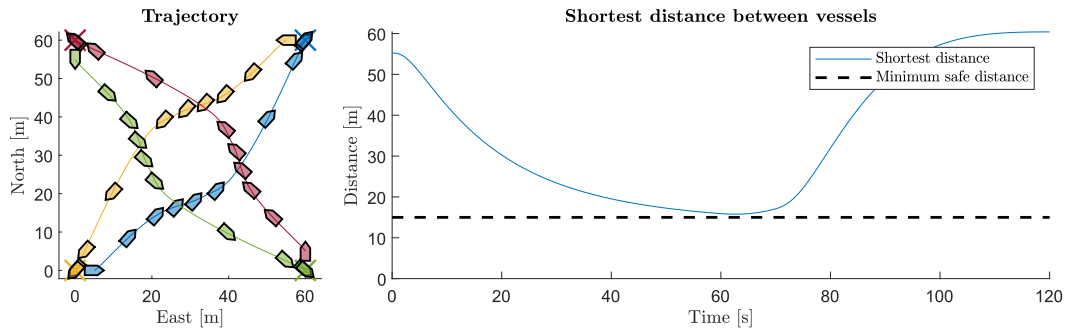


(a) Algorithm (22) on four *milliAmpere* vessels

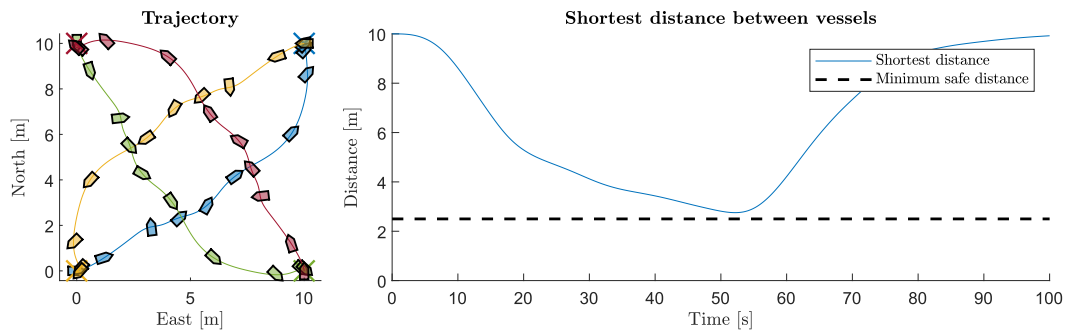


(b) Algorithm (22) on four drillships

Fig. 2: Simulations of the control allocation algorithm (22)

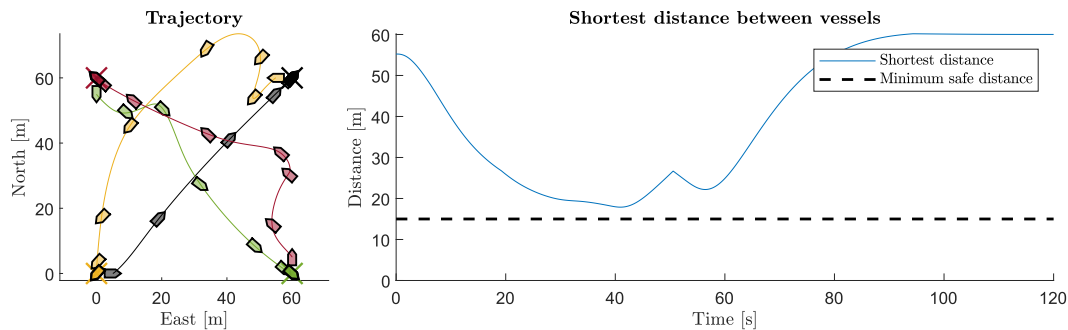


(a) Algorithm (24) on four *milliAmpere* vessels

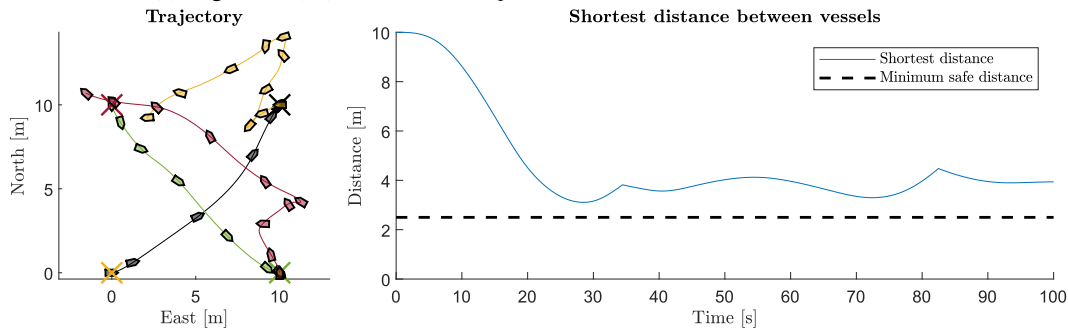


(b) Algorithm (24) on four drillships

Fig. 3: Simulations of the modified control allocation algorithm (24)



(a) Algorithm (24) on four *milliAmpere* vessels with one uncontrolled vessel



(b) Algorithm (24) on four drillships with one uncontrolled vessel

Fig. 4: Simulations of the modified control allocation algorithm (24) with one uncontrolled vessel (plotted in black)

- [5] Y. Kuwata, M. T. Wolf, D. Zargitsky, and T. L. Huntsberger, "Safe Maritime Autonomous Navigation With COLREGS, Using Velocity Obstacles," *IEEE Journal of Oceanic Engineering*, vol. 39, no. 1, pp. 110–119, Jan. 2014.
- [6] A. Lazarowska, "Ship's Trajectory Planning for Collision Avoidance at Sea Based on Ant Colony Optimisation," *The Journal of Navigation*, vol. 68, no. 2, pp. 291–307, Mar. 2015.
- [7] D. Fox, W. Burgard, and S. Thrun, "The Dynamic Window Approach to Collision Avoidance," *IEEE Robotics Automation Magazine*, vol. 4, no. 1, pp. 23–33, Mar. 1997.
- [8] I. B. Hagen, D. K. M. Kufalor, E. F. Brekke, and T. A. Johansen, "MPC-based Collision Avoidance Strategy for Existing Marine Vessel Guidance Systems," in *Proc. 2018 IEEE International Conference on Robotics and Automation*, May 2018, pp. 7618–7623.
- [9] X. Sun, G. Wang, Y. Fan, D. Mu, and B. Qiu, "Collision Avoidance Using Finite Control Set Model Predictive Control for Unmanned Surface Vehicle," *Applied Sciences*, vol. 8, no. 6, p. 926, Jun. 2018.
- [10] Y. Kuriki and T. Namerikawa, "Formation Control with Collision Avoidance for a Multi-UAV System Using Decentralized MPC and Consensus-based Control," *SICE Journal of Control, Measurement, and System Integration*, vol. 8, no. 4, pp. 285–294, 2015.
- [11] L. Dai, Q. Cao, Y. Xia, and Y. Gao, "Distributed MPC for Formation of Multi-agent Systems with Collision Avoidance and Obstacle Avoidance," *Journal of the Franklin Institute*, vol. 354, no. 4, pp. 2068–2085, Mar. 2017.
- [12] G. P. Roussos, D. V. Dimarogonas, and K. J. Kyriakopoulos, "3D Navigation and Collision Avoidance for a Non-holonomic Vehicle," in *Proc. 2008 American Control Conference*, Jun. 2008, pp. 3512–3517.
- [13] A. Mujumdar and R. Padhi, "Reactive Collision Avoidance Using Nonlinear Geometric and Differential Geometric Guidance," *Journal of Guidance, Control, and Dynamics*, vol. 34, no. 1, pp. 303–311, Jan. 2011.
- [14] E. Squires, P. Pierpaoli, and M. Egerstedt, "Constructive Barrier Certificates with Applications to Fixed-Wing Aircraft Collision Avoidance," in *Proc. 2nd IEEE Conference on Control Technology and Applications*, Aug. 2018, pp. 1656–1661.
- [15] M. Igarashi and H. Nakamura, "Collision Avoidance Assist Control for Two-wheel Vehicle Robots by Control Barrier Function," in *Proc. 2018 International Automatic Control Conference*, Nov. 2018, pp. 1–6.
- [16] M. Z. Romdony and B. Jayawardhana, "Stabilization with Guaranteed Safety Using Control Lyapunov–Barrier Function," *Automatica*, vol. 66, pp. 39–47, Apr. 2016.
- [17] E. A. Basso, E. H. Thyri, K. Y. Pettersen, M. Breivik, and R. Skjetne, "Safety-Critical Control of Autonomous Surface Vehicles in the Presence of Ocean Currents," in *Proc. 4th IEEE Conference on Control Technology and Applications*, Aug. 2020, pp. 396–403.
- [18] A. D. Ames, J. W. Grizzle, and P. Tabuada, "Control Barrier Function Based Quadratic Programs with Application to Adaptive Cruise Control," in *53rd IEEE Conference on Decision and Control*, Dec. 2014, pp. 6271–6278.
- [19] R. Hedjar and M. Bounkhel, "An Automatic Collision Avoidance Algorithm for Multiple Marine Surface Vehicles," *International Journal of Applied Mathematics and Computer Science*, vol. 29, no. 4, pp. 759–768, Dec. 2019.
- [20] A. D. Ames, S. Coogan, M. Egerstedt, G. Notomista, K. Sreenath, and P. Tabuada, "Control Barrier Functions: Theory and Applications," in *Proc. 18th European Control Conference*, Jun. 2019, pp. 3420–3431.
- [21] M. W. Oppenheimer, D. B. Doman, and M. A. Bolender, "Control Allocation for Over-actuated Systems," in *Proc. 14th Mediterranean Conference on Control and Automation*, Jun. 2006, pp. 1–6.
- [22] O. Härkegård, "Dynamic Control Allocation Using Constrained Quadratic Programming," *Journal of Guidance, Control, and Dynamics*, vol. 27, no. 6, pp. 1028–1034, 2004.
- [23] T. A. Johansen, T. I. Fossen, and S. P. Berge, "Constrained Nonlinear Control Allocation with Singularity Avoidance Using Sequential Quadratic Programming," *IEEE Transactions on Control Systems Technology*, vol. 12, no. 1, pp. 211–216, Jan. 2004.
- [24] E. H. Thyri, E. A. Basso, M. Breivik, K. Y. Pettersen, R. Skjetne, and A. M. Lekkas, "Reactive Collision Avoidance for ASVs Based on Control Barrier Functions," in *Proc. 4th IEEE Conference on Control Technology and Applications*, 2020, pp. 380–387.
- [25] T. I. Fossen, *Handbook of Marine Craft Hydrodynamics and Motion Control*. John Wiley & Sons, May 2011.
- [26] T. A. Johansen and T. I. Fossen, "Control Allocation—A Survey," *Automatica*, vol. 49, no. 5, pp. 1087–1103, May 2013.
- [27] A. A. Pedersen, "Optimization Based System Identification for the milliAmpere Ferry," 2019, Master's thesis, Norwegian University of Science and Technology (NTNU). [Online]. Available: <http://hdl.handle.net/11250/2625699>
- [28] J. Bjørnø, "Thruster-Assisted Position Mooring of C/S Inocecat I Drillship," 2016, Master's thesis, Norwegian University of Science and Technology (NTNU). [Online]. Available: <http://hdl.handle.net/11250/2402895>